DYNAMICS OF GLOBALLY COUPLED NOISY FITZHUGH-NAGUMO NEURON ELEMENTS

J.A. Acebrón, A.R. Bulsara, and W.-J. Rappel

We study the noisy FitzHugh-Nagumo model in the presence of an external sinusoidal driving force. We derive a Fokker-Planck equation for both the single element and for the globally coupled system. We introduce an efficient way to numerically solve this Fokker-Planck equation and show that the external driving force leads to a classical resonance when its frequency matches the underlying systems frequency. This resonance is also investigated analytically by exploiting the different timescales in the problem. Agreement between the analytical results and numerical results is excellent and reveals the existence of a stochastic bifurcation.

To Vadim Anishchenko, on the occasion of his sixtieth birthday

1. Introduction

The FitzHugh-Nagumo model (FHN) is a simplified version of the celebrated Hodgkin-Huxley model [1], which describes the firing mechanism in a excitable nerve cell. In the FHN, the dynamics of the nerve cell has been reduced to two variables: a fast, activation, variable and a slow, recovery, variable [2]. Due to its relative simplicity, the FHN and its extensions has been studied extensively. Both single neurons and populations of diffusively coupled neurons have been investigated. In addition, the periodically driven FHN, where either the slow or the fast equation contains a time-periodic driving term, has received considerable attention [3-7]. Moreover, as the FHN displays a rich phase diagram that includes excitable, oscillatory and bistable regimes, it has become a «workhorse» in the field of pattern formation (see e.g. [8,9]).

In this paper, we investigate the FHN in the presence of noise and a probe signal. In addition to studying the single element, we examine the effect of coupling the FHN elements in a global fashion. Particular attention is paid to the classical resonance effect that can arise when a system with an underlying frequency is driven by a probe signal [4,10].

2. Model equations

Let us start with the most general form of the FHN model:

$$dx/dt = Ax^3 + Bx^2 + Cx + Hy + I + \xi,$$

$$dy/dt = Ex + Fy + G, \tag{1}$$

where ξ's are Gaussian white noises, with $\langle\xi(t)\rangle=0$, $\langle\xi(t)\xi(t')\rangle=2D\delta(t-t')$ and where A through G are parameters that determine the dynamics of the system. To make the treatment in this paper as general as possible all relevant expressions will be derived using the above set of equations. However, when presenting the results of numerical calculations, we have chosen to limit ourselves here to the investigation of the FHN in its more conventional notation:

$$\alpha dx/dt = x(x-a)(1-x) - y + \xi,$$

$$dy/dt = x - py - b, \tag{2}$$

where α is typically taken to be small.

In order to study the properties of the stochastic differential equation in (1), we start by deriving the Fokker-Planck equation (FPE) for the density probability, which is given by:

$$\partial\rho/\partial t = D\partial^2\rho/\partial x^2 - \partial/\partial x[(Ax^3+Bx^2+Cx+Hy+I)\rho] -$$

$$- \partial/\partial y[(Ex+Fy+G)\rho], \tag{3}$$

which has to be accompanied by initial and boundary data (decay to zero as $x\to\pm\infty$, $y\to\pm\infty$, with sufficiently high rate), and the normalization condition

$$\int_{-\infty}^{\infty}\int_{-\infty}^{\infty} dxdy\rho(x,y,t) = 1. \tag{4}$$

In the following, we are interested in finding solutions of the FPE for large time. This search is greatly facilitated by the fact that the FPE has a unique stationary solution. This can be seen by noting that there exists a Lyapunov function (see [11] and references therein). It then follows that such a stationary solution is unique and globally stable. For parameters values for which analytical progress is difficult to achieve one has to resort to numerics. Direct simulation of the Langevin equations (1), as has been commonly done in the FHN repertoire, can be computationally intensive. For reasonably accurate results one typically has to average over many realizations. This is particularly the case for systems close to a bifurcation point where one has to distinguish between different stable solutions and for systems where the noise is large. Numerical solutions of the FPE, on the other hand, can be obtained much faster. Rather then using a finite difference scheme we have used an efficient spectral method for which we expand the density probability ρ using a basis of Hermite polynomials

$$\rho(x,y,t) = \Sigma_{n=0}^{\infty}r_n^m(t)H_n(x)H_m(y)e^{-x^2}e^{-y^2}. \tag{5}$$

Note that this expansion satisfies the boundary conditions, and the normalization condition with $r_0^0=1/\pi$.

Let us insert Eq. (5) into the FPE (3). We then obtain the following hierarchy of coupled ordinary differential equations for $r_n^m(t)$.

$$\dot{r}_n^m = [\, ^3/_2 An^2 + Cn + Fm]r_n^m + [B(n - ^1/_2)+I]r_{n-1}^m +$$

$$+ [D + ^3/_4A(n - 1) + ^1/_2 C]r_{n-2}^m + (B/4)r_{n-3}^m + (A/8)r_{n-4}^m + Bn(m+1)r_{n+1}^m +$$

$$+ An(n+1)(n+2)r_{n+2}^m + Gr_n^{m-1} + (F/2)r_n^{m-2} + ^1/_2(H+E)r_{n-1}^{m+1} + E(n+1)r_{n+1}^{m-1}, \tag{6}$$

$$n = 0,1...,\infty, \quad m = 0,1...,\infty,$$

where $\langle x \rangle$, and $\langle y \rangle$ are given by

$$\langle x \rangle = \int_{-\infty}^{\infty}\int_{-\infty}^{\infty} dxdy x\rho\,(x,y,t) = \pi r_1^0, \tag{7}$$

$$\langle y \rangle = \int_{-\infty}^{\infty}\int_{-\infty}^{\infty} dxdy y\rho(\,x,y,t) = \pi r_0^1. \tag{8}$$
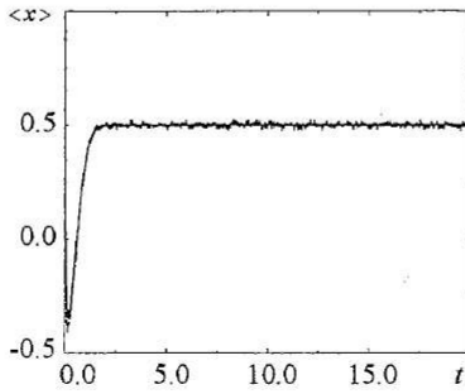

Fig. 1. Comparison between the numerical solution of the Langevin equations (dashed line; averaged over $m=500$ realizations) and the solution of the Fokker-Planck equation (solid line) by the spectral method with $N=M=7$ coefficients. Parameters are $D=0.01, b=0.5, p=1, \alpha=0.05$

The numerical method consists of truncating the infinite hierarchy of first-order, coupled nonlinear differential equations, for a reasonable number of modes $n=0,...,N$, and $m=0,...,M$, setting $r_{N+1}^{M+1}=0$. We have compared the numerical solution obtained via the Fokker-Planck approach, to the solution of the Langevin equations, obtained by averaging over a large number of realizations. In Fig. 1, we plot the first moment $\langle x \rangle$ as a function of time, obtained numerically by solving the Langevin equations (1) and by solving the FPE using the above-described spectral method. The spectral method (with $N=M=7$ moments) is seen to provide excellent agreement with the more conventional and time-consuming technique based on numerically integrating the coupled stochastic differential equations (1).

Following this preamble, we start with an extension of the model equations (1) to describe a system of globally linearly coupled FitzHugh-Nagumo elements. Global coupling is also most amenable (of all the possible coupling schemes) to theoretical treatment. We will couple the elements in the following global fashion:

$$dx_i/dt = Ax_i^3 + Bx_i^2 + Cx_i + Hy_i + I + K/N \sum_{j=1}^{N} (x_j - x_i) + \xi_i, \tag{9}$$

$$dy_i/dt = Ex_i + Fy_i + G, \quad i = 1,...,N. \tag{10}$$

With this type of coupling, the FPE for the perfectly synchronized system is identical to the FPE of a single element.

We are interested in the analytical investigation of the Langevin dynamics above, for the case of very large N. A neat picture of such a case can be given by the limiting-model obtained when $N \to \infty$ (thermodynamic limit). In this limit, it is well known [12,13] that models with mean-field coupling are described by an evolution equation for the one-particle probability density. This can be seen by noting that the hierarchy of equations for all the multiparticle probability densities can be closed by assuming molecular chaos. In such a way, the one-system probability density $\rho(x,y,t)$ is asymptotically in the limit, $N \to \infty$, the solution of the following nonlinear Fokker-Planck equation:

$$\partial\rho/\partial t = D\partial^2\rho/\partial x^2 - \partial/\partial x[(Ax^3 + Bx^2 + Cx + Hy + K(\bar{x} - x) + I)\rho] - \partial/\partial y[(Ex + Fy + G)\rho], \tag{11}$$

where

$$\bar{x} = \int_{-\infty}^{\infty}\int_{-\infty}^{\infty} dxdy x\rho\,(x,y,t). \tag{12}$$

112

The hierarchy (6) now becomes:

$$\dot{r}_n^m = \left(\tfrac{3}{2} An^2 + Cn + Fm - Kn\right)r_n^m + \left[B\left(n - \tfrac{1}{2}\right) + I + \pi Kr_1^0\right]r_{n-1}^m +$$

$$+ \left[D + \tfrac{3}{4} A(n-1) + \tfrac{1}{2}C - K/2\right]r_{n-2}^m + (B/4)r_{n-3}^m + (A/8)r_{n-4}^m + Bn(m+1)r_{n+1}^m +$$

$$+ An(n+1)(n+2)r_{n+2}^m + Gr_n^{m-1} + (F/2)r_n^{m-2} + \tfrac{1}{2}(H+E)r_{n-1}^{m+1} + E(n+1)r_{n+1}^{m-1}, \tag{13}$$

$$n = 0,\ldots,\infty, \quad m = 0,\ldots,\infty.$$

Note that now the hierarchy consists of a system of coupled first-order nonlinear differential equations.

In Fig. 2, we have compared the numerical solution obtained via the nonlinear Fokker-Planck approach to the solution of the Langevin equations for a large number of FHN oscillators (N=5000). The solution of the FPE, corresponding to $N \to \infty$, provides excellent agreement with the finite N case and shows that N=5000 is already close to infinity for all practical purposes.
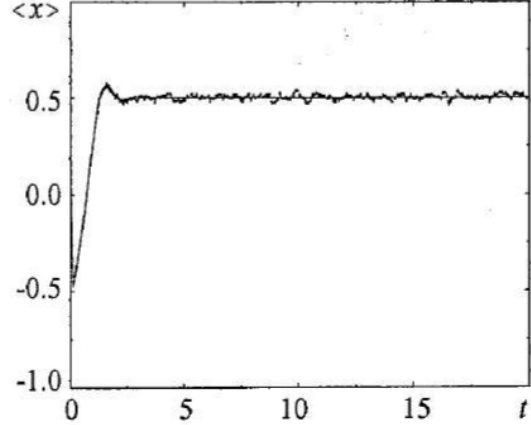

Fig. 2. Comparison between solution obtained by means of FPE (solid line), and direct numerical simulation of the Langevin equations (dashed line) for N=5000 oscillators. Parameters are as in Fig. 1, and K=1

3. Bifurcation analysis

To investigate the bifurcations in the noisy case it is worthwhile to determine the underlying frequency of the system. One way of determining this frequency is to compute $\langle x \rangle$ from the Langevin equations and evaluate its time dependence. Unfortunately, this is computationally very costly. On the other hand, $\langle x \rangle$ calculated from the FPE, which offers a computationally superior way to characterize the system, does not display a time-dependent behavior for a single FHN oscillator. Therefore, an alternative way of finding the frequency needs to be employed. Fortunately, as we will see below, including an external time-sinusoidal «probe» signal leads to a classical resonance which can be used to determine the underlying frequency [4]. We will consider an external signal that has a time-sinusoidal component $G=G_0+q\sin(\omega_p t)$ in (1) (or, equivalently, $b=b_0+q\sin(\omega_p t)$ in (2)).

To illustrate the effect of the probe signal, we first performed Langevin simulations and calculated $\langle y \rangle$. In Fig. 3 we have plotted the power spectrum of this quantity, for three different probe signals; two of them with frequencies ω_p that differs significantly from and one that is very close to the underlying frequency. The power spectrum was obtained by averaging 100 timeseries of 2^{23} timesteps each. The figure illustrates clearly that for a probe signal frequency that matches the broad peak (corresponding to the, in general, non-sinusoidal running oscillations) in the power spectrum of the unprobed system, the signal is amplified. Thus, adding a probe signal gives us a tool to investigate the dynamics of the noisy system. On the other hand, it is worthwhile to exploit such a result to study the bifurcations in our noisy system. In Fig. 3, a, and b, we show the results for two different values of the noise strength. For small noise strength (Fig. 3, a), the peak in the powerspectrum reaches a maximum for non-zero values of the probing frequency while for larger noise strengths (Fig. 3, b) this peak is reached for ω_p=0. Thus, there is a
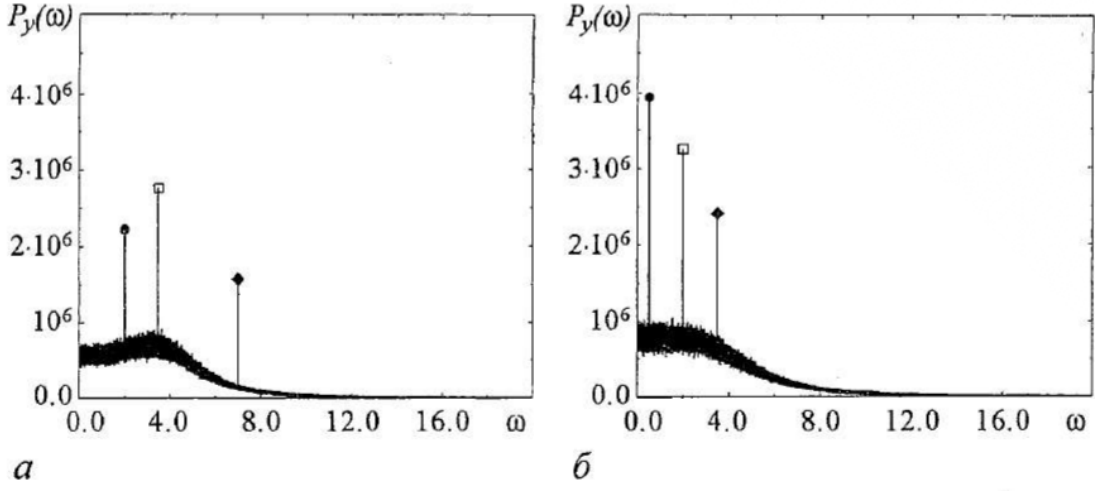
Fig. 3. Power spectrum of the variable y for three different values of the probe signal, and noise strength; (a) ω_p=2.0, 3.5, 7.0, D=0.003, and (b) ω_p=0.5, 2.0, 3.5, D=0.005. Simulations done by using the Langevin equations. Other parameters are b_0=0.5, p=1, q=0.01, and α=0.05

qualitative change in the powerspectrum and in the dynamics of the system, which can be interpreted as the signature of a bifurcation.

Analytical progress by means of the Fokker-Planck equation can be made if we consider a small amplitude signal, $q=\varepsilon Q$, where $\varepsilon \ll 1$. The resulting FPE can then be analyzed via the method of multiple scales. Thus, Eq. (3) contains terms with two different time scales. It is then to be expected that an appropriate asymptotic method will be able to capture the long-time behavior of ρ. This may be achieved by introducing fast and slow timescales as follows:

$$\tau = t/\varepsilon, \quad t = t. \tag{14}$$

We look for a distribution function satisfying the boundary condition according to the Ansatz:

$$\rho(x,y,t;\varepsilon) = \sum_{n=0}^{2} \rho^{(n)}(x,y,t,\tau)\varepsilon^n + O(\varepsilon^3). \tag{15}$$

From (15), the average of x is given by

$$\langle x \rangle = \langle x \rangle^{(0)} + \varepsilon \langle x \rangle^{(1)} + O(\varepsilon^2), \tag{16}$$

where

$$\langle x \rangle^{(j)} = \int_{-\infty}^{\infty} \int_{-\infty}^{\infty} dx dy x \, \rho^{(j)}(x,y,t). \tag{17}$$

The average of y is given by similar equations. Inserting (15) into (3), we obtain the following hierarchy of equations for $\rho^{(j)}$:

$$\partial\rho^{(0)}/\partial\tau = 0, \tag{18}$$

$$\partial\rho^{(1)}/\partial\tau = D\partial^2\rho^{(0)}/\partial x^2 - \partial/\partial x[(Ax^3 +Bx^2+Cx+Hy+I)\rho^{(0)}] -$$
$$- \partial/\partial y[(Ex+Fy+G_0)\rho^{(0)}] - \partial\rho^{(0)}/\partial t, \tag{19}$$

$$\partial\rho^{(2)}/\partial\tau = D\partial^2\rho^{(1)}/\partial x^2 - \partial/\partial x[(Ax^3 +Bx^2+Cx+Hy+I)\rho^{(1)}] -$$
$$- \partial/\partial y[(Ex+Fy+G_0)\rho^{(1)}] - \partial\rho^{(1)}/\partial t - Q\sin(\omega_p t)\partial\rho^{(0)}/\partial y, \tag{20}$$

114

where the normalization conditions

$$\int_{-\infty}^{\infty}\int_{-\infty}^{\infty} \rho^{(n)}(x,y,t)\,dx\,dy = \delta_{0n} \tag{21}$$

follows from (4). Eq. (18) implies that $\rho^{(0)}$ is independent of τ. Then, the terms in the right side of (19) which do not have τ-dependent coefficients give rise to secular terms (unbounded on the τ-time scale). The condition that no secular terms should appear is

$$D\partial^2\rho^{(0)}/\partial x^2 - \partial/\partial x[(Ax^3 +Bx^2+Cx+Hy+I)\rho^{(0)}] -$$
$$- \partial/\partial y[(Ex+Fy+G_0)\rho^{(0)}] - \partial\rho^{(0)}/\partial t = 0. \tag{22}$$

This equation should be solved for $\rho^{(0)}$ together with the normalization condition and initial condition data. Note that this problem is equivalent to solving the FPE (3) without the probe signal as the effects of the probe signal appear first when calculating the first-order correction, $\rho^{(1)}$.

To calculate these first-order corrections, we again impose the condition that no secular terms appear and that the right-hand side of (20) vanishes. The resulting equation is:

$$D\partial^2\rho^{(1)}/\partial x^2 - \partial/\partial x[(Ax^3 +Bx^2+Cx+Hy+I)\rho^{(1)}] -$$
$$- \partial/\partial y[(Ex+Fy+G_0)\rho^{(1)}] - \partial\rho^{(1)}/\partial t - Q\sin(\omega_p t)\partial\rho^{(0)}/\partial y = 0. \tag{23}$$

The analysis of the equation above can be readily accomplished in Fourier space. Fourier transforming Eq. (23), we obtain

$$i\omega\hat{\rho}^{(1)} = D\partial^2\hat{\rho}^{(1)}/\partial x^2 - \partial/\partial x[(Ax^3 +Bx^2+Cx+Hy+I)\hat{\rho}^{(1)}] -$$
$$- \partial/\partial y[(Ex+Fy +G_0)\hat{\rho}^{(1)}] -i(Q/2)\partial/\partial y[\hat{\rho}^{(0)}(\omega+\omega_p) - \hat{\rho}^{(0)}(\omega-\omega_p)], \tag{24}$$

where

$$\hat{\rho}^{(j)}(x,y,\omega) = \int_{-\infty}^{\infty}dt\,e^{-i\omega t}\, \rho^{(j)}(x,y,t), \tag{25}$$

$$\langle\hat{x}\rangle^{(j)} = \int_{-\infty}^{\infty}\int_{-\infty}^{\infty}dx\,dy\, x\hat{\rho}^{(j)}(x,y,t), \tag{26}$$

$$j = 0,1. \tag{27}$$

The equation (24) should be solved for $\hat{\rho}^{(1)}$ together with $\int_{-\infty}^{\infty}\int_{-\infty}^{\infty}dx\,dy\,\hat{\rho}^{(1)}=0$. Since $\rho^{(0)}$ evolves to a stationary solution for long-time (i.e. $\hat{\rho}^{(0)}=\delta(\omega)f(\delta_1,\delta_2)$), we find that $\hat{\rho}^{(1)}=0$ is the only solution of (24), unless $\omega=\pm\omega_p$. Then, (24),(27) imply that

$$\hat{\rho}^{(1)} = \eta^+(x,y)\,\delta(\omega-\omega_p) + \eta^-(x,y)\delta(\omega+\omega_p). \tag{28}$$

Inserting (28) in Eq. (24), we obtain two uncoupled equations for η^+, and η^-. These can be solved, by expanding $\eta^\pm$ in Hermite polynomials,

$$\eta^\pm(x,y) = \Sigma_{n=0}^{\infty}\Sigma_{m=0}^{\infty}(T^\pm)_n{}^m H_n(x)H_m(y)e^{-x^2}e^{-y^2}, \tag{29}$$

and solving the corresponding nonlinear systems of equations for the coefficients $(T^\pm)_n{}^m$. Once we obtain $(T^\pm)_n{}^m$, we can calculate $\langle\hat{x}\rangle^{(1)}$ from Eq. (27). Notice that $\hat{\rho}(+\omega_p)=\hat{\rho}^*(-\omega_p)$, by taking the complex conjugate in (24), and (27). Then it follows from (28), and (29) that $(T^+)_n{}^m=((T^-)_{-n}{}^{-m})^*$. Therefore we conclude that $\langle\hat{x}\rangle^{(1)}(-\omega_p)=(\langle\hat{x}\rangle^{(1)})^*(+\omega_p)$, and the
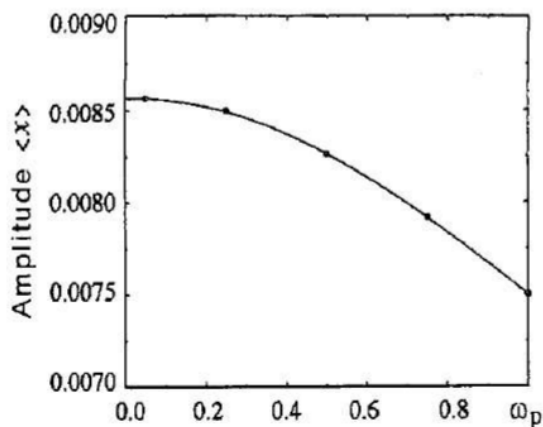
Fig. 4. Comparison between the theoretical results and the numerical simulations, marked by symbols. Parameters are $D=0.05$, $b_0=0.3$, $p=1$, $q=0.01$, and $\alpha=0.05$
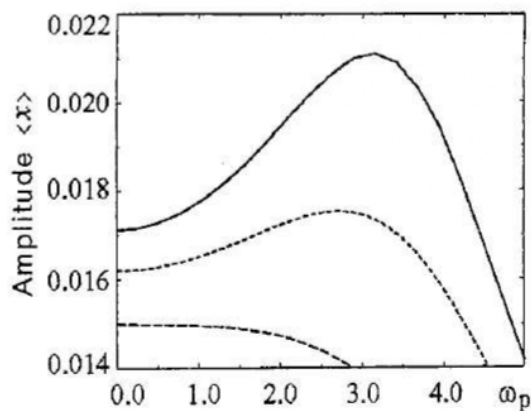

Fig. 5. $\langle x \rangle$ versus the frequency of the probe signal for different values of the noise strength: $D=0.002$ (solid line); 0.003 (dot line); 0.005 (dashed). Results obtained by means of the theory for a single FHN. Parameters are $b_0=0.5$, $p=1$, $q=0.01$, and $\alpha=0.05$

inverse Fourier transform yields

$$\langle x \rangle^{(1)}(t) = 2\text{Re}(\langle \hat{x} \rangle^{(1)}(\omega_p)) \cos(\omega_p t) - 2\text{Im}(\langle \hat{x} \rangle^{(1)}(\omega_p))\sin(\omega_p t). \tag{30}$$

Knowing $\langle x \rangle^{(1)}(t)$, its amplitude can be readily computed, and the result is

$$A_{\langle x \rangle} = 2[\langle \hat{x} \rangle^{(1)}(\langle \hat{x} \rangle^{(1)})^*]^{1/2} + O(\epsilon^2). \tag{31}$$

In Fig. 4, we plotted the numerical solution and the theoretical approximation (31), showing a remarkable agreement with the theoretical results corresponding to the first-order expansion. It should be noticed, however, that the amplitude of the probe signal considered here is small, $q=0.01$. For increasing strength of the amplitude, higher orders in the expansion may be required. Once $\rho^{(1)}$ is known, it is also straightforward to find the successive terms in the expansion. Without entering into a detailed study, some general features can easily be drawn from the hierarchy of equations for $\rho^{(j)}$. Similarly to the analysis for $\hat{\rho}^{(1)}$, and by taking into account that $\hat{\rho}^{(1)}$ is a function exclusively of $\omega \pm \omega_p$, it is
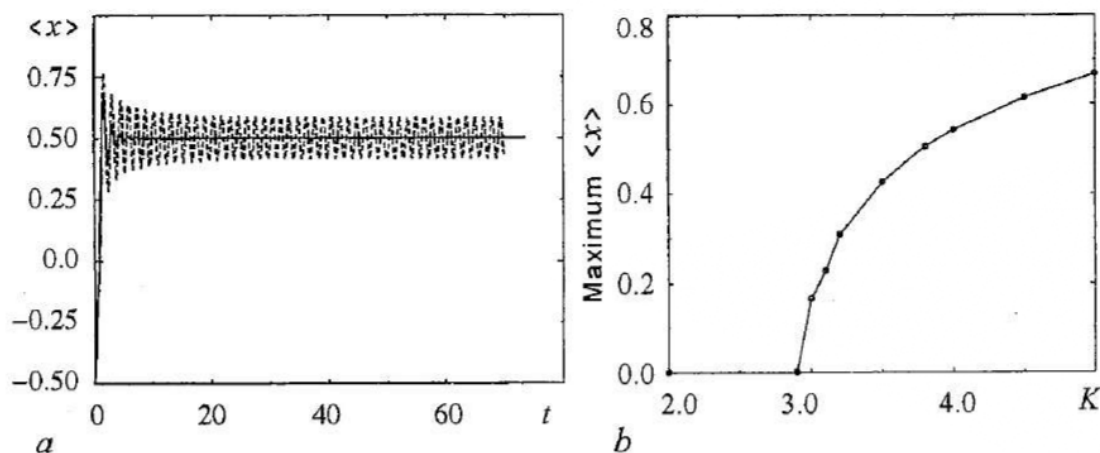

Fig. 6. (a) $\langle x \rangle$ versus time for two different values of the coupling $K=2$ (solid line) and $K=3$ (dot line), showing a clear bifurcation. (b) Amplitude of $\langle x \rangle$ vs coupling for a fixed level of noise. Parameters are as in Fig. 5

straightforward to prove that $\hat{\rho}^{(2)}=0$ is the only solution unless $\omega=0;\pm2\omega_p$. In general, successive terms will depend on higher harmonics of the main frequency ω_p.

By applying the theory above, we were able to obtain the amplitude of $\langle x \rangle$ as function of the frequency of the probe signal, shown in Fig. 5. It should be noticed that for increasing noise levels, the peak moves to smaller values of ω and then disappears. This was already observed in Fig. 3 and can be interpreted as a sign of a stochastic bifurcation.

We now investigate the case of coupled FHN elements for which the dynamical response exhibits bifurcations, even in the absence of a probe signal. The bifurcation, of the Hopf-type, is shown in Fig. 6 where we have plotted the amplitude of $\langle x \rangle$ vs coupling for a fixed level of noise. Below some critical coupling strength, the system is not synchronized and the solution of the FPE is stationary. On the other hand, above this critical coupling strength, the system synchronizes and exhibits a time-dependent behavior.

The inclusion of a probe signal will elicit a time-dependent solution of the FPE, even when the system *without* the probe signal has a stationary solution. The amplitude of the response ($\langle x \rangle$) depends critically on the frequency of the probe signal as is shown in Fig. 7. In contrast to similar coupled systems (see e.g. [10]), increasing the coupling does not lead to the «death» of the oscillatory region and the optimal frequency actually increases as the coupling is increased. The position and amplitude of the peak in Fig. 7 depends on the coupling strength. For $K=0$ the response curve does not exhibit a peak showing that there is no underlying frequency in the problem. Increasing K produces an underlying frequency which appears as a peak in the curve. Notice that for $K>2.9$ the system will synchronize in the absence of a probe signal. This, then, leads to a response that has two principal frequencies: the frequency arising from the Hopf bifurcation and the probe frequency.
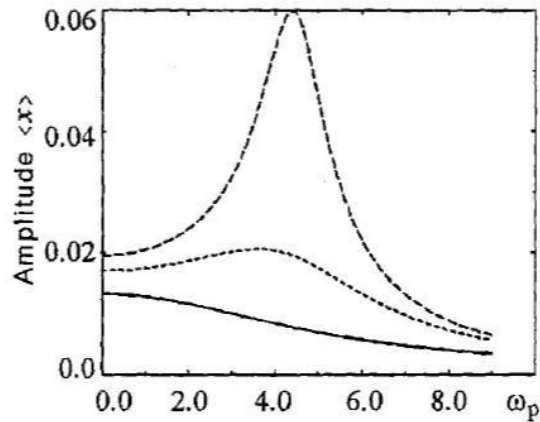

Fig. 7. Amplitude of $\langle x \rangle$ versus the frequency of the probe signal for three different values of the coupling strength $K=0$ (solid line) and $K=1$ (dot line), $K=2$ (dashed line). Parameters are as in Fig. 5

4. Summary

In this paper, we have investigated the single and globally coupled FHN model in the presence of noise and an injection signal. We have derived a FPE for the system and have shown that we can solve this FPE efficiently by using a suitably chosen expansion. We find that there is a classical resonance effect when the frequency of the probe signal approaches the one of the underlying system. We also characterize this resonance by separating the fast and slow time scales in the problem and find that, for small driving amplitudes, the agreement between numerical and analytical results is excellent. Finally, we reveal the existence of a stochastic bifurcation (see Fig. 1 and Fig. 3), manifested by the qualitative change of the peak location in the curves of $A_{\langle x \rangle}$ vs ω_p.

Future work will include the further characterization of the bifurcation we observed. Note that the bifurcation we found is different from the one found in earlier work [14]. We plan to address these differences in a future publication. In addition, we plan to investigate further the response of the globally coupled system to a probe signal. Particular attention will be paid to the possibility that, upon inclusion of an input signal, a

population can become synchronized and can produce a large output signal. By varying the intrinsic parameters, including the coupling constant, the response can thus be «tuned» at different frequencies. Whether or not real neurons make use of this mechanism remains to be seen.

References

1. *Hodgkin A.L. and Huxley A.F.* // *J. Physiol.* (London). 1952. Vol. 117. P. 500.
2. See, e.g., *Keener J. and Sneyd J.* Mathematical Physiology. Springer-Verlag, Berlin, 1998.
3. *Longtin A.* // Chaos, Soliton, Fractal. 2000. Vol. 11. P. 1835.
4. *Massanés S.R. and Pérez Vicente C.J.* // Int. J. Bif. Chaos. 1999. Vol. 9. P. 2295; Phys. Rev. E. 1999. Vol. 59. P. 4490.
5. *Lindner B., and Schimansky-Geier L.* // Phys. Rev. E. 1999. Vol. 60. P. 7270.
6. *Pikovsky A.S., and Kurths J.* // Phys. Rev. Lett. 1997. Vol. 78. P. 775.
7. *Kurrer C. and Schulten K.* // Phys. Rev. E. 1995. Vol. 51. P. 6213.
8. *Winfree A.T.* // Chaos. 1991. Vol. 1. P. 303.
9. *Hagberg A. and Meron E.* // Nonlinearity.1994. Vol. 7. P. 805.
10. *Acebrón J.A., Bulsara A.R., Rappel W-J.,* submitted for publication.
11. *Risken H.* The Fokker-Planck equation: Methods of Solution and Applications. Springer Verlag, Berlin, 1996.
12. *Desai R.C., and Zwanzing R.* // J. Stat. Phys. 1978. Vol. 19. P. 1.
13. *Shiino M.* // Phys. Lett. A. 1985. Vol. 112A. P. 302; Phys. Rev. A. 1987. Vol. 36. P. 2393.
14. *Tanabe S., and Pakdaman K.* // Phys. Rev. E. 2001. Vol. 63. 031911.

Department of Physics
University of California, San Diego, USA
SPA WAR Systems Center,
San Diego, USA

ДИНАМИКА ГЛОБАЛЬНО СВЯЗАННЫХ НЕЙРОННЫХ ЭЛЕМЕНТОВ ФИТЦХЬЮ - НАГУМО В ПРИСУТСТВИИ ШУМА

J.A. Acebrón, A.R. Bulsara, W.-J. Rappel

Мы изучаем модель ФитцХью - Нагумо при наличии шума и внешнего синусоидального воздействия. Записываем уравнение Фоккера - Планка для отдельного элемента и для глобально связанной системы. Представляем эффективный способ численного решения этого уравнения Фоккера - Планка и показываем, что внешнее воздействие приводит к классическому резонансу, при котором его частота совпадает с собственной частотой системы. Этот резонанс также исследуется аналитически путем использования различных временных

масштабов. В задаче наблюдается хорошее соответствие между аналитическими и численными результатами и обнаружено существование стохастической бифуркации.

J.A. Acebrón is a scientific worker of SPAWAR Systems Center Code D363, 49590 Lassing Road, RM A341 San Diego, CA 92152-6147, USA.

Dr. Bulsara is one of the leading scientists at the US Navy's Space and Naval Warfare Systems Center (SPAWAR) laboratory in San Diego, California. His major field of interest is applications of stochastic cooperative phenomena in coupled nonlinear systems.
E-mail: bulsara@spawar.navy.mil

W.-J. Rappel is a scientific worker of SPAWAR Systems Center Code D363, 49590 Lassing Road, RM A341 San Diego, CA 92152-6147, USA.